

pubs.acs.org/JACS Article

Boron-Methylated Dipyrromethene as a Green Light Activated Type I Photoinitiator for Rapid Radical Polymerizations

Kun-You Chung and Zachariah A. Page*



Cite This: J. Am. Chem. Soc. 2023, 145, 17912-17918



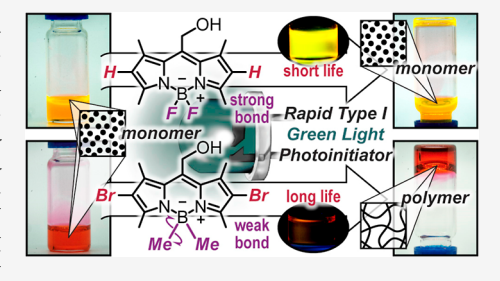
ACCESS I

III Metrics & More

Article Recommendations

Supporting Information

ABSTRACT: Unimolecular (Type I) radical photoinitiators (PIs) have transformed the chemical manufacturing industry by enabling (stereo)lithography for microelectronics and emergent 3D printing technologies. However, the reliance on high energy UV-violet light (≤420 nm) restricts the end-use applications. Herein, boronmethylated dipyrromethene (methylated-BODIPY) is shown to act as a highly efficient Type I radical PI upon irradiation with low energy green light. Using a low intensity (~4 mW/cm²) light emitting diode centered at 530 nm and a low PI concentration (0.3 mol %), acrylic-based resins were polymerized to maximum conversion in ~10 s. Under equivalent conditions (wavelength, intensity, and PI concentration), state-of-the-art visible light PIs Ivocerin and Irgacure 784 show no



appreciable polymerization. Spectroscopic characterization suggests that homolytic β -scission at the boron—carbon bond results in radical formation, which is further facilitated by accessing long-lived triplet excited states through installment of bromine. Alkylated-BODIPYs represent a new modular visible light PI platform with exciting potential to enable next generation manufacturing and biomedical applications where a spectrally discrete, low energy, and thus benign light source is required.

■ INTRODUCTION

Visible light has emerged as a promising stimulus to drive polymerizations for a variety of applications, 1-8 particularly in the biomedical and advanced manufacturing (e.g., 3D printing) arenas. This arises in part from the inherent spatiotemporal control, high penetration depth, low energy, and discrete absorption it offers to enable benign and wavelength-selective fabrication of multifunctional soft materials. 10 In particular, the discrete absorption of low energy photons in the visible to near infrared spectral region results in deeper light penetration into biological materials (e.g., tissue) and a reduction in phototoxicity relative to higher energy ultraviolet (UV) light. 11 As a result, the development of efficient visible light photoinitiating systems will enable biomaterials fabrication, such as 3D cell encapsulation for tissue engineering applications. However, a major hurdle limiting the implementation of visible light driven polymerizations is its low efficiency relative to UV light driven processes.^{3,8} This arises from a difference in the mechanism to generate initiating species for polymerization, such as radicals, which has been predominantly restricted to bimolecular processes for long wavelength light (≥500 nm) (i.e., Type II, photoredox) and unimolecular processes for short wavelength light (<500 nm) (i.e., Type I, photolysis). 12-14 In-turn, the requirement for cocatalysts such as tertiary amines, 15 iodonium salts, 16 and/or borate salts 17,18 in Type II processes are intrinsically diffusion limited, slowing overall photocuring rates, increasing complexity and cost, and potentially decreasing biocompatibility of the concomitant resin formulations. 15,19 Therefore, long wavelength (>500 nm) Type I

photoinitiators offer a compelling alternative, yet remain elusive.

A classic Type I photoinitiator that absorbs visible light (~405 nm) is bisacylphosphine oxide (BAPO), which has been employed industrially in lithography and 3D printing owing to its high radical generation efficiency (Figure 1). 20,21 In analogy to traditional UV-activated aryl ketones, acylphos-

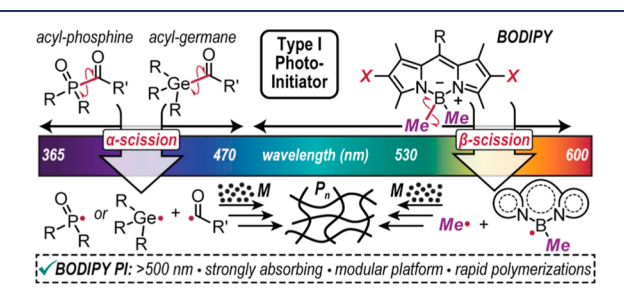


Figure 1. Juxtaposition of traditional aryl ketone UV- to blue-light activated Type I radical photoinitiators undergoing α -scission and present green-light activated boron-methylated BODIPY photoinitiator undergoing β -scission to induce rapid monomer (M) to polymer (P_n) formation.

Received: May 23, 2023 Published: August 4, 2023





phine oxides undergo homolytic α -scission (C–P bond) after photoexcitation, ^{20–22} directly producing a high concentration of radicals capable of inducing rapid acrylate polymerization (i.e., curing). However, aryl ketone absorption occurs via a spin-forbidden $n-\pi^*$ electronic transition, resulting in low molar absorptivity in the visible region (~405 nm). Efforts to red-shift the absorption have been made by replacing the carbonyl oxygen atom with sulfur or selenium to manipulate the n-bonding energy, $^{23-25}$ or by replacing the α -carbon with germanium (commercial product Ivocerin). 26,27 However, absorption peak maxima in these derivatives remain confined to wavelengths <450 nm, and their challenging syntheses^{24,25} and potential toxicity ^{19,28} have hindered widespread use as single-component photoinitiators in photocurables. Additional examples of visible light induced polymerizations include those employing titanocene derivatives (commercial product Irgacure 784),^{29,30} palladium diimine catalysts,³¹ phenyl iodonium π -conjugated boron dipyrromethene (BODIPY) salts,³² and thiocarbonylthio chain transfer agents used in controlled radical (photoiniferter) polymerization. 33,34 Still, absorption peak maxima are <500 nm and/or have low molar absorptivity above 500 nm (<1000 M⁻¹ cm⁻¹), necessitating the use of high light intensities (>50 mW/cm²) and/or photoinitiator concentrations (>2 wt %) to achieve photopolymerizations on timescales relevant to lithography and 3D printing (\sim seconds).

Inspired by UV-light induced β -scission observed in N-heterocyclic carbene boranes, $\frac{35-38}{20}$ blue-light (440 nm) induced β -scission of boracenes, ³⁹ and recent utility of electron-rich boryl radicals as nucleophiles in synthetic chemistry⁴⁰⁻⁴² it was hypothesized that boron-functionalized variants of BODIPY fluorophores could provide a novel Type I photoinitiator platform for rapid and efficient free radical polymerization. Moreover, it was recently shown that boronethylated BODIPY could be used as a turn-on fluorescent sensor upon irradiation with a high intensity blue laser (488 nm, ≥ 28 W/cm²), resulting in substitution of the ethyl functionality, although the mechanism was not reported.⁴ Herein, it was discovered that boron-methylated BODIPY (≤0.6 wt %) acts as a highly efficient Type I photoinitiator upon exposure to low intensity green light (~530 nm, <5 mW/ cm²) to induce rapid acrylate polymerizations (<20 s to max conversion) (Figure 1).

RESULTS AND DISCUSSION

A series of BODIPY photoinitiators (PIs) were designed to increase the excited-state lifetime (halogenation) and potentially result in bond homolysis (boron methylation), while maintaining ease of synthetic accessibility (Figure 2A). 1,44 To start, meso-methylacetate BODIPY was synthesized from 2,4dimethylpyrrole with 2-chloro-2-oxoethyl-acetate, followed by reaction with boron trifluoride etherate (Scheme S1). Subsequent hydrolysis of acetate with sodium hydroxide gave BODIPY-F-H. Alternatively, boron methylation was accomplished by treating meso-methyl acetate BODIPY with methyl magnesium bromide, which simultaneously substituted the fluorine atoms and cleaved the ester to provide an alcohol, yielding BODIPY-Me-H. Bromination of the BODIPY-F-H and -Me-H derivatives was accomplished in an analogous manner using N-bromosuccinimide (NBS) to provide BODIPY-F-Br and -Me-Br, respectively. Overall, the synthetic procedure was modular and only required three facile steps,

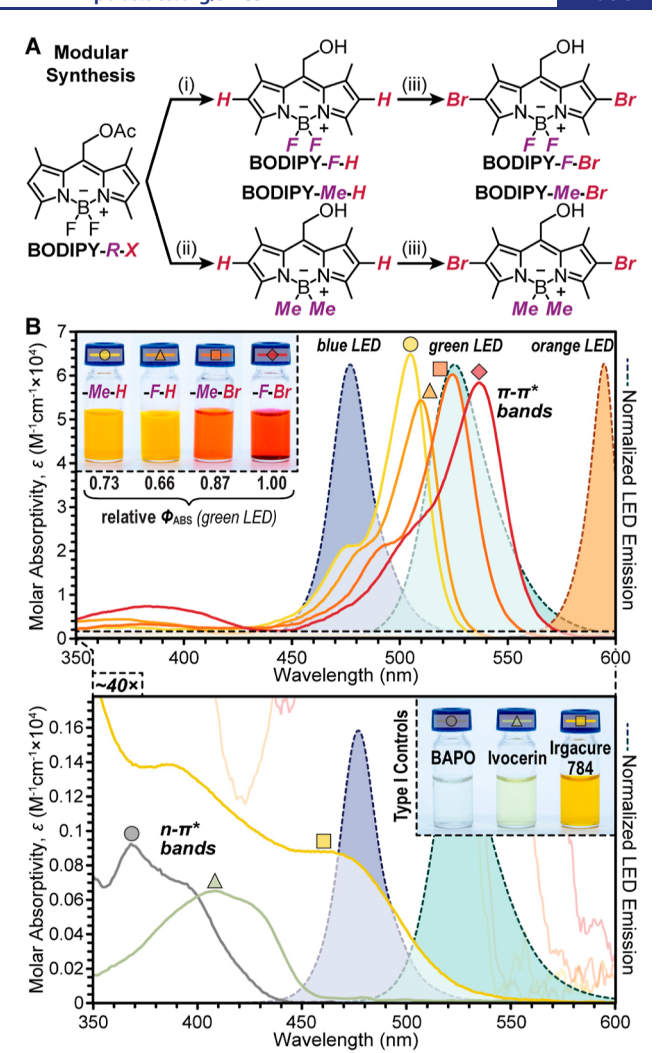


Figure 2. (A) BODIPY PI synthesis. (i) 1 M NaOH(aq), $CH_2Cl_2/MeOH$ (1:2), 3 h; (ii) CH_3MgBr , CH_2Cl_2 , 30 min; (iii) NBS, CH_2Cl_2 , 1 h. (B) UV–vis absorption spectra of BODIPY PIs (top) and commercial Type I PIs (bottom) in CH_3CN (5 μ M). Relevant LED emission traces underlaid. Insets: images of corresponding PIs in CH_3CN (2 mM).

making it more accessible relative to those for alternative visible light PIs, such as acylgermanes (e.g., Ivocerin^{26,27}).

Upon isolation, it was immediately evident that each compound had a distinct absorption profile, as they were visually different colors in solution (Figure 2B, inset). To ultimately assess the reactivity of each BODIPY derivative, it was deemed necessary to characterize molar absorptivity (ε), which was accomplished using UV-vis absorption spectroscopy (Figures 2B and S21). Values were comparable in both dilute solution (5 μ M in CH₃CN, 1 cm pathlength, Figure 2B) and in a representative resin formulation described later (0.1 mol % in isobornyl acrylate, 25 μ m pathlength, Figure S21). From this analysis, the π - π * absorption bands for all derivatives were found to peak between 500 and 550 nm, with ε values in excess of 50,000 M⁻¹ cm⁻¹. Notably, methylation resulted in a ~5-10 nm hypsochromic (blue-)shift, while bromination resulted in a ~20-25 nm bathochromic (red-)shift (Table S1). Subsequently, the spectral emission profile for blue (470 nm), green (530 nm), and orange (590 nm) LEDs used herein were characterized to determine the extent of overlap with the different BODIPY

absorption profiles. Quantification of the relative number of LED photons absorbed (Φ_{ABS}) was accomplished by normalizing to the derivative with the greatest amount of overlap, BODIPY-F-Br. This provided Φ_{ABS} values of 0.73, 0.66, 0.87, and 1.0 for BODIPY-Me-H, -F-H, -Me-Br, and -F-Br, respectively.

To place these derivatives into context, they were directly compared with state-of-the-art industrial Type I PIs. Specifically, UV-vis absorption spectra were collected for BAPO, Ivocerin, and Irgacure 784 and overlaid with the same blue and green LEDs (Figure 2B, bottom). Owing to the "forbidden" $n-\pi^*$ transition that results in radical formation among these PIs, their S_0 to S_1 ε values in the visible region were >40× lower compared to the BODIPYs. Considering the blue LED with only the commercial PIs, BAPO, Ivocerin, and Irgacure 784 had Φ_{ABS} values of 0.05, 0.1, and 1.0, respectively. However, in looking at the green LED, BAPO had negligible absorption, and relative to BODIPY-F-Br, Ivocerin and Irgacure 784 had Φ_{ABS} values of <0.001 and 0.013, respectively (Table S2). Thus, BODIPY-F-Br absorbed >1000× and 77× more green LED photons relative to Ivocerin and Irgacure 784, respectively. Therefore, based solely on absorption (i.e., holding reaction quantum yields equal) one would expect significantly greater radical formation and concomitantly faster rates of polymerization for a Type I BODIPY PI.

To test this conjecture, the utility of different BODIPY derivatives as Type I PIs to induce free-radical polymerizations was examined using real-time Fourier transform infrared (RT-FTIR) spectroscopy in an attenuated total reflection (ATR) mode (Figure 3A, and Supporting Information for details). Isobornyl acrylate (IBOA) was selected as a model system, owing to its biorenewable sourcing and low volatility. Monomer to polymer conversion was determined by monitoring the peak at \sim 770 cm⁻¹ (C=C vinylic stretch⁴⁵) during LED irradiation. Initial experiments were performed with 0.3 mol % BODIPY and a green LED intensity of 4 mW/ cm², which are conditions relevant to contemporary projection-based 3D printing (e.g., digital light processing⁶ and liquid crystal display 46). Fully formed resins were purged with an inert gas (e.g., argon) to remove oxygen as a potential radical and triplet excited state scavenger. Under these conditions, the methylated BODIPY derivatives resulted in the fastest polymerization rates (r_n) , with BODIPY-Me-Br being $\sim 16 \times$ faster than BODIPY-Me-H (Figure 3B). Specifically, r_p values were 0.007 M/s (0.1% C=C conversion/s), 0.017 M/s (0.3%/s), and 0.33 M/s (6.5%/s) for BODIPY-F-Br, -Me-H, and -Me-Br, respectively (no polymerization was observed for BODIPY-F-H). Versatility in monomer scope was demonstrated by polymerizing isobornyl methacrylate, 2-hydroxyethyl acrylate, and carbitol acrylate (Figures S22-S24, and Table S3). All polymerizable resins showed an excellent temporal response and good stability, as no measurable conversion occurred in the dark, corresponding to the first 15 s of RT-FTIR spectroscopy measurements. After turning the LED on, the resin containing BODIPY-Me-Br as the PI reached maximum monomer conversion in ~10 s (~80% for neat IBOA due to vitrification). Furthermore, long term stability testing was performed by storing resin comprised of IBOA and BODIPY-Me-Br (0.3 mol %) at room temperature in the dark and measuring photopolymerization kinetics via RT-FTIR spectroscopy each week over the course of one month (Figure S25). Notably, no significant change in r_p , t_{50} , and maximum

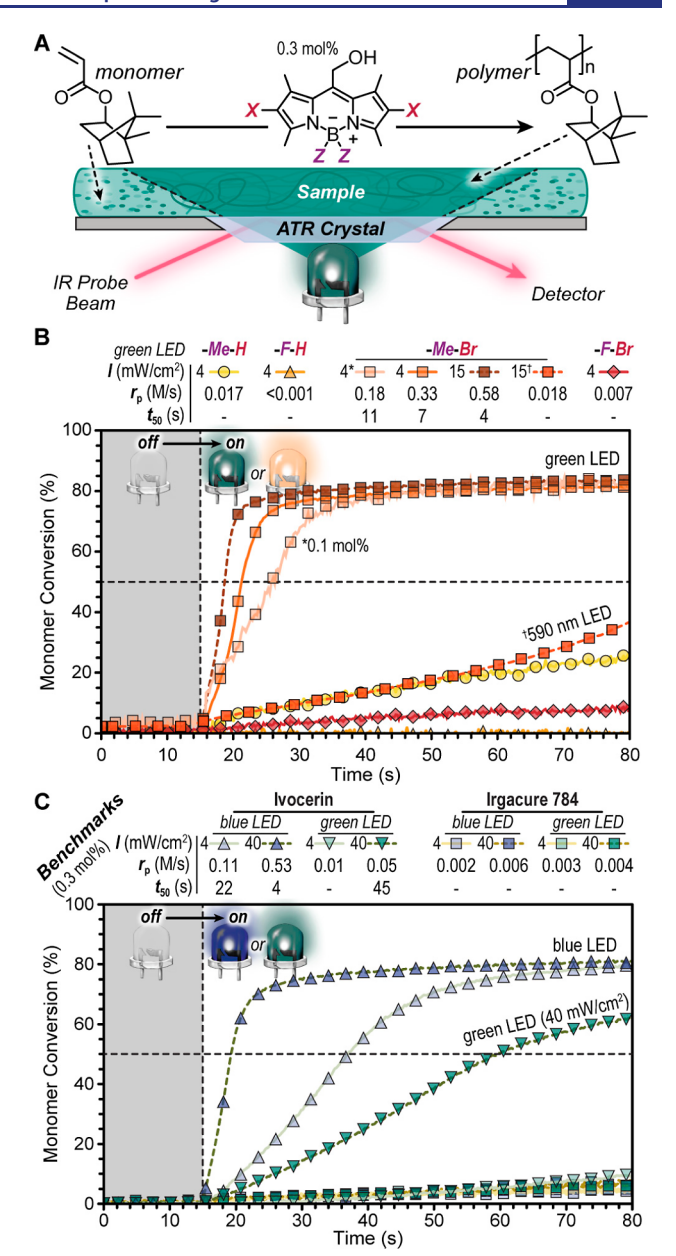


Figure 3. (A) Illustration of the in situ monitoring of monomer to polymer conversion with ATR-FTIR. (B) Plot of monomer to polymer conversion versus time for BODIPY PIs upon exposure to a green LED centered at 530 nm († or an orange LED centered at 590 nm) in comparison to (C) commercial Type I PIs upon exposure to a green (530 nm) or blue (470 nm) LED. All PI concentrations were 0.3 mol % (* or 0.1 mol % as noted).

monomer conversion was observed, which demonstrates good BODIPY photoinitiator stability.

Examining the champion BODIPY-Me-Br PI further revealed that rapid green light-induced polymerizations to max monomer conversion were possible using a concentration of 0.1 mol % (3× lower than previous) (Figure 3B). Under this condition, an $r_{\rm p}$ of 0.18 M/s (3.6%/s) and a time to 50% conversion (t_{50}) of 11 s (relative to 7 s for 0.3 mol %) were observed. Note that t_{50} values are provided as a simple benchmark for comparison. Additionally, increasing the light intensity from 4 to 15 mW/cm² resulted in an $r_{\rm p}$ of 0.58 M/s (12%/s) and a t_{50} of 4 s, making it nearly 2× faster. Finally, an orange LED centered at 590 nm was employed at 15 mW/cm²,

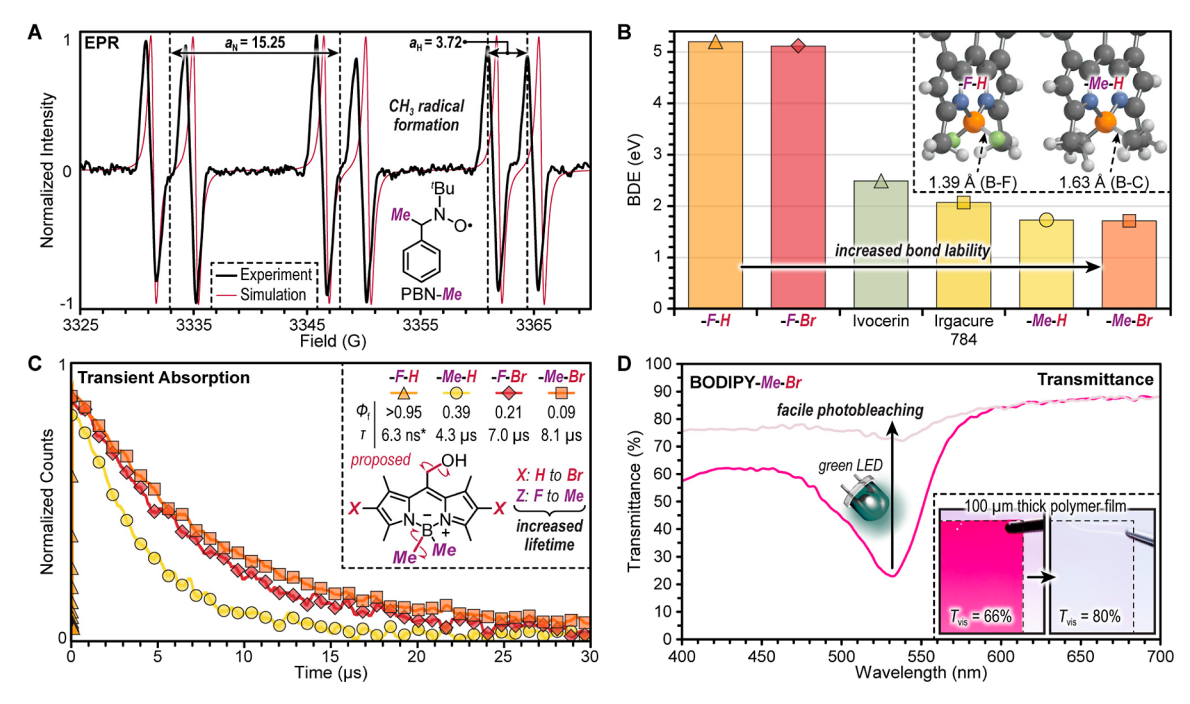


Figure 4. (A) EPR spectrum for a green-light irradiated sample that contained BODIPY-Me-Br and N-tert-butyl-α-phenylnitrone (PBN) (black trace), and simulated result of PBN-Me (red trace). (B) Bond dissociation enthalpy (BDE) values determined computationally using density functional theory. Inset: 3D structures with B–F and B–C bond lengths indicated. (C) Excited state lifetime characterization by transient absorption spectroscopy. Inset provides fluorescence quantum yield (Φ_f) values obtained using fluorescence spectroscopy and excited state lifetime (τ). *Data for BODIPY-F-H was obtained using time-correlated single photon counting fluorescence spectroscopy due to lack of a triplet signal in transient absorption. (D) Visible light transmittance (T_{vis}) of a polymer film prepared using BODIPY-Me-Br as the photoinitiator right after preparation and after an extended irradiation with a green LED centered at 530 nm.

which resulted in an $r_{\rm p}$ of 0.018 M/s (0.4%/s), comparable to that measured for BODIPY-Me-H with the green LED at 4 mW/cm². Notably, under equimolar conditions of BODIPY-Me-Br, the $r_{\rm p}$ was ~30× lower in going from green to orange light irradiation (both at 15 mW/cm²), yet the relative number of orange photons absorbed was nearly 10,000× lower (Figure S21). This suggests that the photopolymerization efficiency is considerably higher under the orange light conditions, which could arise from competitive side-reactions that occur at higher excited-state and/or radical densities.

The BODIPY PIs were benchmarked against state-of-the-art commercial PIs, Ivocerin and Irgacure 784, which have been reported to operate under blue and green light irradiation (Figure 3C).^{27,29} Using equimolar quantities of PI (0.3 mol %) in IBOA, samples were irradiated with 4 or 40 mW/cm² blue and green LEDs, again monitoring with RT-FTIR spectroscopy. Under green light irradiation, only the sample containing Ivocerin exposed at an intensity of 40 mW/cm² displayed an appreciable r_p of 0.05 M/s (1.0%/s) and a t_{50} of 45 s, despite having a Φ_{ABS} of 0.07 relative to Irgacure 784 (i.e., absorbing ~14× fewer green LED photons). Irradiating instead with a blue LED revealed again only polymerizations occurring with Ivocerin and not Irgacure under the conditions and timeframe (\sim 60 s) examined. With a blue LED intensity of 4 mW/cm², the samples containing Ivocerin had an r_p of 0.11 M/s (2.2%/ s) and a t_{50} of 22 s. Increasing the intensity to 40 mW/cm² resulted in an r_p of 0.53 M/s (11%/s) and a t_{50} of 4 s, which was comparable to that observed for BODIPY-Me-Br irradiated with 15 mW/cm² using a green LED. Overall, at equivalent concentrations the BODIPY PIs significantly outperformed current visible light PIs using lower energy and intensity LEDs.

At this stage, the hypothesis was put forward that free radical polymerization was caused by light-induced homolytic β scission at the boron-carbon bond (B-CH₃) for the methylated BODIPYs. This bond is considered β as it is separated from π -conjugation by one atom, boron, which is sp³-hybridized. Additionally, the small extent of polymerization observed for resins with BODIPY-F-Br was rationalized by inefficient homolytic β -scission at the meso-methyl C–O bond, as previously reported for coumarin-based photocages. 47 Next, a series of spectroscopic and computational characterization techniques were employed to determine the mechanism (Figure 4). First, electron paramagnetic resonance (EPR) spectroscopy was used with spin-trapping experiments to confirm the radical character and associated chemical composition of the fragmented products. The spin-trapping agent N-tert-butyl-α-phenylnitrone (PBN, 10 mM) was dissolved together with BODIPY-Me-Br (5 mM) in CH₂Cl₂, and the mixture was irradiated with the green LED for 5 min. Characterization of the resulting mixture by EPR spectroscopy revealed one predominant PBN-adduct with hyperfine coupling constants characteristic of methylation ($a_N = 15.25$, $a_{\rm H} = 3.72$), ⁴⁸ and in agreement with simulations (Figure 4A). This suggested that methyl radicals were being formed, and the initiation mechanism by •CH3 was also reported in previous studies. 49,50 Additionally, size exclusion chromatography on poly(IBOA) samples prepared using BODIPY-Me-Br had a clear UV absorption (350 nm) signal (Figure S31). This indicated boryl-radical initiation given the lack of other 350 nm absorbing components in the initial mixture. Further evidence of β -scission at the B-C bond was obtained using nuclear magnetic resonance spectroscopy and liquid chromatographymass spectrometry characterization, which revealed formation

of B-OCH₃ and B-(OH)₂ adducts when irradiating the BODIPY PI in methanol and water, respectively (Figures S32-

In order for the purported B–C β -scission to occur, the bond dissociation enthalpy (BDE) would need to be lower than the input energy, which for 530 nm photons is ~2.4 eV. Notably, this matches both the spectral (Figures 2B and S21) and electrochemical (Figures S26-S29 and Table S4) energy gaps for the BODIPY PIs. Using density functional theory, BDE values for the different BODIPY derivatives and Type I PI benchmarks were estimated. While the classic BODIPY structures bearing B-F bonds showed a high BDE of ~5 eV, replacing the fluorine atoms with methyl groups resulted in a dramatic decrease in BDE to ~1.7 eV, irrespective of the presence or absence of bromine (Figure 4B). This significant decrease in BDE was also supported by the larger bond length for B-C (1.63 Å) relative to B-F (1.39 Å) (Figure 4B, inset). Additionally, the BDE values for the methylated BODIPY PIs were found to be lower in comparison to the benchmarks, Ivocerin and Irgacure 784, which were 2.5 and 2.1 eV, respectively. Despite the low BDE value, the BODIPY PIs were stable and qualitatively easy to handle on the bench without prematurely inducing polymerization.

Next, we sought to better understand the role of bromine in the observed photopolymerization rate enhancement. This was accomplished by characterizing excited state dynamics using a combination of fluorescence and transient absorption spectroscopies (Figures 4C and S35-S43). Initially, fluorescence quantum yield (Φ_f) values were determined using rhodamine 6G as a standard, finding that BODIPY-F-H was considerably more fluorescent ($\Phi_f = 0.95$) relative to BODIPY-Me-H, -F-Br, and -Me-Br; $\Phi_{\rm f}$ = 0.39 \pm 0.06, 0.21 \pm 0.05, and 0.09 \pm 0.02, respectively (Figure 4C inset, Figure S35, and Table S1). Transient absorption spectroscopy was then employed to examine the non-radiative excited-state dynamics, which revealed long-lived populations that were attributed to spintriplet states (Figure 4C). Specifically, the excited state lifetime (τ) values for BODIPY-Me-H, -F-Br, and -Me-Br were found to be 4.3, 7.0, and 8.1 μ s (Figure 4C inset, Figure S41–S43, and Table S1). Notably, τ is ~1000× longer for the triplet excited states relative to the corresponding singlet excited states (\sim 1–6 ns), as characterized using time-correlated single photon counting fluorescence spectroscopy (Figures S37–S40 and Table S1). Based on this result, the competitive nonradiative decay pathway was attributed to intersystem crossing, which would indicate that triplet yield increases in going from BODIPY-Me-H, -F-Br, and -Me-Br. Overall, the PIs possessing longer triplet lifetimes correlate with faster polymerization rates. In accord, it was hypothesized that accessing a higher population of long-lived triplet excited states increases the likelihood for B–C β -scission to occur per photon absorbed, providing a useful design principle.

As a final proof-of-concept relevant to photocurable technologies (e.g., 3D printing), BODIPY-Me-Br was employed as a PI to rapidly prepare a polymer network (Figure 4D). A resin comprising 50 wt % IBOA (monomer), 50 wt % trimethylolpropane triacrylate (crosslinker), and the BODIPY PI (0.3 mol %) was placed into a 100 µm gap between glass slides, followed by irradiation with the green LED under ambient conditions (~5 min). Separating the glass slides provided a pink plastic film with a visible light transmittance $(T_{\rm vis})$ of 66%. The color from the film was almost completely removed (bleached, $T_{vis} = 80\%$) upon

extended irradiation with green light (525 nm, 0.8 W/cm², 2.5 min), providing an avenue to access colorless and transparent plastics using low energy green light.

CONCLUDING REMARKS

In summary, BODIPY-Me-X represents a novel, efficient visible light photoinitiator platform to induce rapid radical polymerizations relevant to the photochemistry community, with particularly pertinent applications in photocurables (e.g., coatings, adhesives, (stereo)lithography, etc.). Based on results presented herein, we postulate that B-C β -scission in alkylated-BODIPY derivatives is a general phenomenon, and thus has exciting potential for improvement owing to the modularity of this chromophore. For example, enhancements in radical generation efficiency may be possible through further tailoring the composition of the "X" and "Z" groups presented, while π -extended BODIPYs have the potential to enable longer wavelength, red light (~1.9 eV) photoinitiation via a Type I mechanism. As a result, it is anticipated that these derivatives will enable applications in the biomedical and advanced manufacturing arenas where selectively absorbed, benign visible light is paramount, such as in the development of next generation cell-laden tissue scaffolds for disease modeling and multimaterial 3D printing to create soft actuators and stretchable electronics.

ASSOCIATED CONTENT

Supporting Information

The Supporting Information is available free of charge at https://pubs.acs.org/doi/10.1021/jacs.3c05373.

Materials and methods, synthesis, and spectroscopic characterization (PDF)

AUTHOR INFORMATION

Corresponding Author

Zachariah A. Page – Department of Chemistry, The University of Texas at Austin, Austin, Texas 78712, United States; orcid.org/0000-0002-1013-5422; Email: zpage@ utexas.edu

Author

Kun-You Chung – Department of Chemistry, The University of Texas at Austin, Austin, Texas 78712, United States

Complete contact information is available at: https://pubs.acs.org/10.1021/jacs.3c05373

The authors declare no competing financial interest.

ACKNOWLEDGMENTS

The authors acknowledge primary support by the National Science Foundation under Grant no. MSN-2107877 (K.-Y.C. and Z.A.P.; synthesis and characterization, supervision, and writing). Partial support was provided by the Robert A. Welch Foundation under Grant no. F-2007 (Z.A.P.; partial materials and supplies support) and Research Corporation for Science Advancement via a Cottrell Scholars Award #28184 (Z.A.P.; partial materials and supplies support). We acknowledge Prof. Sean Roberts and his research group for the use of a Magnitude Instruments enVISion spectrometer for nanosecond transient absorption measurements.

ABBREVIATIONS

PI photoinitiator

 $\begin{array}{lll} \mbox{BODIPY} & \mbox{boron dipyrromethene} \\ \mbox{BAPO} & \mbox{bisacylphosphine oxide} \\ \mbox{NBS} & \mbox{N-bromosuccinimide} \\ \mbox{$\Phi_{\rm ABS}$} & \mbox{relative photons absorbed} \end{array}$

RT-FTIR real-time Fourier transform infrared

ATR attenuated total reflection

IBOA isobornyl acrylate t_{50} time to 50% conversion

EPR electron paramagnetic resonance PBN N-tert-butyl- α -phenylnitrone BDE bond dissociation enthalpy $\Phi_{\rm f}$ fluorescence quantum yield τ excited state lifetime $T_{\rm vis}$ visible light transmittance

REFERENCES

- (1) Chung, K. Y.; Halwachs, K. N.; Lu, P.; Sun, K.; Silva, H. A.; Rosales, A. M.; Page, Z. A. Rapid Hydrogel Formation via Tandem Visible Light Photouncaging and Bioorthogonal Ligation. *Cell Rep. Phys. Sci.* **2022**, *3*, 101185.
- (2) Jung, K.; Corrigan, N.; Ciftci, M.; Xu, J.; Seo, S. E.; Hawker, C. J.; Boyer, C. Designing with Light: Advanced 2D, 3D, and 4D Materials. *Adv. Mater.* **2019**, 32, 1903850.
- (3) Bao, Y. Recent Trends in Advanced Photoinitiators for Vat Photopolymerization 3D Printing. *Macromol. Rapid Commun.* **2022**, 43, 2200202.
- (4) Bao, Y.; Paunović, N.; Leroux, J. C. Challenges and Opportunities in 3D Printing of Biodegradable Medical Devices by Emerging Photopolymerization Techniques. *Adv. Funct. Mater.* **2022**, 32, 2109864.
- (5) Narupai, B.; Nelson, A. 100th Anniversary of Macromolecular Science Viewpoint: Macromolecular Materials for Additive Manufacturing. ACS Macro Lett. 2020, 9, 627–638.
- (6) Ahn, D.; Stevens, L. M.; Zhou, K.; Page, Z. A. Rapid High-Resolution Visible Light 3D Printing. ACS Cent. Sci. 2020, 6, 1555–1563
- (7) Stafford, A.; Ahn, D.; Raulerson, E. K.; Chung, K.-Y.; Sun, K.; Cadena, D. M.; Forrister, E. M.; Yost, S. R.; Roberts, S. T.; Page, Z. A. Catalyst Halogenation Enables Rapid and Efficient Polymerizations with Visible to Far-Red Light. *J. Am. Chem. Soc.* **2020**, *142*, 14733–14742.
- (8) Bagheri, A.; Jin, J. Photopolymerization in 3D Printing. ACS Appl. Polym. Mater. 2019, 1, 593-611.
- (9) Bonardi, A. H.; Dumur, F.; Grant, T. M.; Noirbent, G.; Gigmes, D.; Lessard, B. H.; Fouassier, J. P.; Lalevée, J. High Performance Near-Infrared (NIR) Photoinitiating Systems Operating under Low Light Intensity and in the Presence of Oxygen. *Macromolecules* **2018**, *51*, 1314–1324.
- (10) Lu, P.; Ahn, D.; Yunis, R.; Delafresnaye, L.; Corrigan, N.; Boyer, C.; Barner-Kowollik, C.; Page, Z. A. Wavelength-Selective Light-Matter Interactions in Polymer Science. *Matter* **2021**, *4*, 2172–2229.
- (11) Ash, C.; Dubec, M.; Donne, K.; Bashford, T. Effect of Wavelength and Beam Width on Penetration in Light-Tissue Interaction Using Computational Methods. *Laser Med. Sci.* **2017**, 32, 1909–1918.
- (12) Chen, M.; Zhong, M.; Johnson, J. A. Light-Controlled Radical Polymerization: Mechanisms, Methods, and Applications. *Chem. Rev.* **2016**, *116*, 10167–10211.
- (13) Dadashi-Silab, S.; Doran, S.; Yagci, Y. Photoinduced Electron Transfer Reactions for Macromolecular Syntheses. *Chem. Rev.* **2016**, *116*, 10212–10275.
- (14) Corrigan, N.; Shanmugam, S.; Xu, J.; Boyer, C. Photocatalysis in Organic and Polymer Synthesis. *Chem. Soc. Rev.* **2016**, *45*, 6165–6212.

- (15) Kowalska, A.; Sokolowski, J.; Bociong, K. The Photoinitiators Used in Resin Based Dental Composite-A Review and Future Perspectives. *Polymers* **2021**, *13*, 470.
- (16) Merritt, E. A.; Olofsson, B. Diaryliodonium Salts: A Journey from Obscurity to Fame. Angew. Chem., Int. Ed. 2009, 48, 9052–9070.
- (17) Jędrzejewska, B.; Pietrzak, M. Applicability of Hemicyanine Phenyltrialkylborate Salts as Free-Radical Photoinitiators in the Visible-Light Polymerization of Acrylate. *J. Appl. Polym. Sci.* **2012**, 123, 3535–3544.
- (18) Zhou, J.; Pitzer, L.; Ley, C.; Rölle, T.; Allonas, X. A highly sensitive photoinitiating system based on pre-associated ion-pairs for NIR radical photopolymerization of optically clear materials. *Polym. Chem.* **2022**, *13*, 6475–6483.
- (19) Popal, M.; Volk, J.; Leyhausen, G.; Geurtsen, W. Cytotoxic and Genotoxic Potential of the Type I Photoinitiators BAPO and TPO on Human Oral Keratinocytes and V79 Fibroblasts. *Dent. Mater.* **2018**, 34, 1783–1796.
- (20) Sluggett, G. W.; Turro, C.; George, M. W.; Koptyug, I. V.; Turro, N. J. (2,4,6-Trimethylbenzoyl)Diphenylphosphine Oxide Photochemistry. A Direct Time-Resolved Spectroscopic Study of Both Radical Fragments. *J. Am. Chem. Soc.* **1995**, *117*, 5148–5153.
- (21) Jockusch, S.; Koptyug, I. V.; McGarry, P. F.; Sluggett, G. W.; Turro, N. J.; Watkins, D. M. A Steady-State and Picosecond Pump-Probe Investigation of the Photophysics of an Acyl and a Bis(Acyl)Phosphine Oxide. *J. Am. Chem. Soc.* **1997**, *119*, 11495–11501.
- (22) Jockusch, S.; Landis, M. S.; Freiermuth, B.; Turro, N. J. Photochemistry and Photophysics of α -Hydroxy Ketones. *Macromolecules* **2001**, 34, 1619–1626.
- (23) Kryman, M. W.; Schamerhorn, G. A.; Hill, J. E.; Calitree, B. D.; Davies, K. S.; Linder, M. K.; Ohulchanskyy, T. Y.; Detty, M. R. Synthesis and Properties of Heavy Chalcogen Analogues of the Texas Reds and Related Rhodamines. *Organometallics* **2014**, *33*, 2628–2640.
- (24) Ichikawa, Y.; Kamiya, M.; Obata, F.; Miura, M.; Terai, T.; Komatsu, T.; Ueno, T.; Hanaoka, K.; Nagano, T.; Urano, Y. Selective Ablation of β -Galactosidase-Expressing Cells with a Rationally Designed Activatable Photosensitizer. *Angew. Chem., Int. Ed.* **2014**, 53, 6772–6775.
- (25) Poronik, Y. M.; Vygranenko, K. V.; Gryko, D.; Gryko, D. T. Rhodols-Synthesis, Photophysical Properties and Applications as Fluorescent Probes. *Chem. Soc. Rev.* **2019**, *48*, 5242–5265.
- (26) Brook, A. G.; Duff, J. M.; Jones, P. F.; Davis, N. R. Synthesis of Silyl and Germyl Ketones. J. Am. Chem. Soc. 1966, 89, 431–434.
- (27) Haas, M.; Radebner, J.; Eibel, A.; Gescheidt, G.; Stueger, H. Recent Advances in Germanium-Based Photoinitiator Chemistry. *Chem.—Eur. J.* **2018**, 24, 8258–8267.
- (28) Spallholz, J. E. On the nature of selenium toxicity and carcinostatic activity. *Free Radical Biol. Med.* **1994**, *17*, 45–64.
- (29) Kitano, H.; Ramachandran, K.; Bowden, N. B.; Scranton, A. B. Unexpected Visible-Light-Induced Free Radical Photopolymerization at Low Light Intensity and High Viscosity Using a Titanocene Photoinitiator. *J. Appl. Polym. Sci.* **2013**, *128*, 611–618.
- (30) Tehfe, M. A.; Lalevée, J.; Morlet-Savary, F.; Graff, B.; Fouassier, J. P. On the Use of Bis(Cyclopentadienyl)Titanium(IV) Dichloride in Visible-Light-Induced Ring-Opening Photopolymerization. *Macromolecules* **2012**, *45*, 356–361.
- (31) Keyes, A.; Dau, H.; Basbug Alhan, H. E.; Ha, U.; Ordonez, E.; Jones, G. R.; Liu, Y. S.; Tsogtgerel, E.; Loftin, B.; Wen, Z.; Wu, J. I.; Beezer, D. B.; Harth, E. Metal-Organic Insertion Light Initiated Radical (MILRad) Polymerization: Photo-Initiated Radical Polymerization of Vinyl Polar Monomers with Various Palladium Diimine Catalysts. *Polym. Chem.* **2019**, *10*, 3040–3047.
- (32) Topa-Śkwarczyńska, M.; Galek, M.; Jankowska, M.; Morlet-Savary, F.; Graff, B.; Lalevée, J.; Popielarz, R.; Ortyl, J. Development of the First Panchromatic BODIPY-Based One-Component Iodonium Salts for Initiating the Photopolymerization Processes. *Polym. Chem.* **2021**, *12*, 6873–6893.
- (33) Hartlieb, M. Photo-Iniferter RAFT Polymerization. *Macromol. Rapid Commun.* **2022**, 43, 2100514.

- (34) Figg, C. A.; Hickman, J. D.; Scheutz, G. M.; Shanmugam, S.; Carmean, R. N.; Tucker, B. S.; Boyer, C.; Sumerlin, B. S. Color-Coding Visible Light Polymerizations to Elucidate the Activation of Trithiocarbonates Using Eosin Y. *Macromolecules* **2018**, *51*, 1370–1376.
- (35) Telitel, S.; Vallet, A. L.; Schweizer, S.; Delpech, B.; Blanchard, N.; Morlet-Savary, F.; Graff, B.; Curran, D. P.; Robert, M.; Lacôte, E.; Lalevée, J. Formation of N-Heterocyclic Carbene-Boryl Radicals through Electrochemical and Photochemical Cleavage of the B-S Bond in N-Heterocyclic Carbene-Boryl Sulfides. *J. Am. Chem. Soc.* 2013, 135, 16938–16947.
- (36) Lalevée, J.; Blanchard, N.; Tehfe, M. A.; Chany, A. C.; Fouassier, J. P. New Boryl Radicals Derived from N-Heteroaryl Boranes: Generation and Reactivity. *Chem.—Eur. J.* **2010**, *16*, 12920–12927.
- (37) Ueng, S. H.; Solovyev, A.; Yuan, X.; Geib, S. J.; Fensterbank, L.; Lacôte, E.; Malacria, M.; Newcomb, M.; Walton, J. C.; Curran, D. P. N-Heterocyclic Carbene Boryl Radicals: A New Class of Boron-Centered Radical. *J. Am. Chem. Soc.* **2009**, *131*, 11256–11262.
- (38) Aubry, B.; Subervie, D.; Lansalot, M.; Bourgeat-Lami, E.; Graff, B.; Morlet-Savary, F.; Dietlin, C.; Fouassier, J. P.; Lacôte, E.; Lalevée, J. A Second-Generation Chameleon N-Heterocyclic Carbene-Borane Coinitiator for the Visible-Light Oxygen-Resistant Photopolymerization of Both Organic and Water-Compatible Resins. *Macromolecules* 2018, *51*, 9730–9739.
- (39) Sato, Y.; Nakamura, K.; Hashizume, D.; Sumida, Y.; Hosoya, T.; Ohmiya, H.; Ohmiya, H. Generation of Alkyl Radical through Direct Excitation of Boracene-Based Alkylborate. *J. Am. Chem. Soc.* **2020**, *142*, 9938–9943.
- (40) Zhao, Q.; Li, B.; Zhou, X.; Wang, Z.; Zhang, F. L.; Li, Y.; Zhou, X.; Fu, Y.; Wang, Y. F. Boryl Radicals Enabled a Three-Step Sequence to Assemble All-Carbon Quaternary Centers from Activated Trichloromethyl Groups. *J. Am. Chem. Soc.* **2022**, *144*, 15275–15285.
- (41) Li, W. D.; Wu, Y.; Li, S. J.; Jiang, Y. Q.; Li, Y. L.; Lan, Y.; Xia, J. B. Boryl Radical Activation of Benzylic C-OH Bond: Cross-Electrophile Coupling of Free Alcohols and CO2via Photoredox Catalysis. J. Am. Chem. Soc. 2022, 144, 8551–8559.
- (42) Nakamura, R.; Yamazaki, T.; Kondo, Y.; Tsukada, M.; Miyamoto, Y.; Arakawa, N.; Sumida, Y.; Kiya, T.; Arai, S.; Ohmiya, H. Radical Caging Strategy for Cholinergic Optopharmacology. *J. Am. Chem. Soc.* **2023**, *145*, 10651–10658.
- (43) Wijesooriya, C. S.; Peterson, J. A.; Shrestha, P.; Gehrmann, E. J.; Winter, A. H.; Smith, E. A. A Photoactivatable BODIPY Probe for Localization-Based Super-Resolution Cellular Imaging. *Angew. Chem.* **2018**, *130*, 12867–12871.
- (44) Slanina, T.; Shrestha, P.; Palao, E.; Kand, D.; Peterson, J. A.; Dutton, A. S.; Rubinstein, N.; Weinstain, R.; Winter, A. H.; Klán, P. In Search of the Perfect Photocage: Structure—Reactivity Relationships in *meso*-Methyl BODIPY Photoremovable Protecting Groups. *J. Am. Chem. Soc.* **2017**, *139*, 15168—15175.
- (45) Uddin, A.; Allen, S. R.; Rylski, A. K.; O'Dea, C. J.; Ly, J. T.; Grusenmeyer, T. A.; Roberts, S. T.; Page, Z. A. Do The Twist: Efficient Heavy-Atom-Free Visible Light Polymerization Facilitated by Spin-Orbit Charge Transfer Inter-System Crossing. *Angew. Chem., Int. Ed.* 2023, 62, No. e202219140.
- (46) Stevens, L. M.; Recker, E. A.; Zhou, K. A.; Garcia, V. G.; Mason, K. S.; Tagnon, C.; Abdelaziz, N.; Page, Z. A. Counting All Photons: Efficient Optimization of Visible Light 3D Printing. *Adv. Mater. Technol.* **2023**, 2300052. Early View
- (47) Takano, M. A.; Abe, M. Photoreaction of 4-(Bromomethyl)-7-(Diethylamino)Coumarin: Generation of a Radical and Cation Triplet Diradical during the C-Br Bond Cleavage. *Org. Lett.* **2022**, 24, 2804–2808.
- (48) Arroyo, C. M.; Kramer, J. H.; Leiboff, R. H.; Mergner, G. W.; Dickens, B. F.; Weglicki, W. A. Spin trapping of oxygen and carbon-centered free radicals in ischemic canine myocardium. *Free Radical Biol. Med.* **1987**, *3*, 313–315.

(49) Fischer, H.; Baer, R.; Hany, R.; Verhoolen, I.; Walbiner, M. 2,2-Dimethoxy-2-phenylacetophenone: photochemistry and free radical photofragmentation. *J. Chem. Soc., Perkin Trans.* **1990**, *2*, 787–798. (50) Hageman, H. J. Photoinitiators for Free Radical Polymerization.

Prog. Org. Coat. 1985, 13, 123-150.